

Incommensurate charge-stripe correlations in the kagome superconductor $\text{CsV}_3\text{Sb}_{5-x}\text{Sn}_x$

Linus Kautzsch,¹ Yuzki M. Oey,¹ Hong Li,² Zheng Ren,² Brenden R. Ortiz,¹ Ram Seshadri,¹ Jacob Ruff,³ Ziqiang Wang,² Ilija Zeljkovic,² and Stephen D. Wilson¹

¹*Materials Department, University of California Santa Barbara, California 93106 United States*

²*Department of Physics, Boston College, Chestnut Hill, MA 02467, USA*

³*CHESS, Cornell University, Ithaca, New York 14853, USA*

(Dated: July 22, 2022)

We track the evolution of charge correlations in the kagome superconductor CsV_3Sb_5 as its parent, long-ranged charge density order is destabilized. Upon hole-doping, interlayer charge correlations rapidly become short-ranged and their periodicity is reduced by half along the interlayer direction. Beyond the peak of the first superconducting dome, the parent charge density wave state vanishes and incommensurate, quasi-1D charge correlations are stabilized in its place. These competing, unidirectional charge correlations demonstrate an inherent electronic rotational symmetry breaking in CsV_3Sb_5 , independent of the parent charge density wave state and reveal a complex landscape of charge correlations across the electronic phase diagram of this class of kagome superconductors. Our data suggest an inherent $2k_f$ charge instability and the phenomenology of competing charge instabilities is reminiscent of what has been noted across several classes of unconventional superconductors.

Charge correlations and the nature of charge density wave (CDW) order within the new class of $AV_3\text{Sb}_5$ ($A=\text{K, Rb, Cs}$) kagome superconductors [1–4] are hypothesized to play a crucial role in the anomalous properties of these compounds. Hints of pair density wave superconductivity [5, 6] as well as signatures of orbital magnetism [7–10] in these compounds are all born out of a central CDW state [11–13]. The CDW order parameter itself is theorized to host both primary, real and secondary, imaginary components [14], each of which thought to play a role in the anomalous properties observed in $AV_3\text{Sb}_5$ compounds.

The real component of the CDW state in $AV_3\text{Sb}_5$ compounds manifests primarily as a 2×2 reconstruction within the kagome plane driven via a $3\mathbf{q}$ distortion into either star-of-David (SoD) or (its inverse) tri-hexagonal (TrH) patterns of order [15]. In-plane $3\mathbf{q}$ distortions are further correlated between kagome layers [11, 16–18], either through correlated phase shifts of the same distortion type between neighboring layers, via alternation between distortion mode types, or a combination of both [19].

The parent CDW state of CsV_3Sb_5 forms as a $2 \times 2 \times 4$ supercell whose average structure is comprised of a modulation between SoD and TrH distortion modes along the interlayer c -axis below $T_{CDW} = 94$ K [17, 20, 21]. Upon cooling, however, the CDW state also shows hints of a staged behavior, suggestive of another coexisting or competing CDW instability. Scanning tunneling microscopy (STM) measurements resolve commensurate, quasi-1D charge stripes that form near $T \approx 60$ K and coexist with the 2×2 in-plane CDW order [12]. Transient reflectivity [22] and Raman measurements [23] also resolve a shift/new modes in the lattice dynamics near this same energy scale. Sb NQR and V NMR measurements further resolve a chemical shift below 60 K [24], demonstrating a structural response to a modified CDW order

parameter—a response potentially driven by a competing CDW instability.

Further supporting the notion of a competing, electronic instability is the rapid suppression of the parent CDW order in CsV_3Sb_5 under moderate pressure [25, 26] or via small levels of hole-substitution [27]. By substituting ≈ 6 % holes per formula unit, the CDW state seemingly vanishes in thermodynamic measurements, while superconductivity undergoes a nonmonotonic response and generates two superconducting domes. The evolution of charge correlations as the parent, three-dimensional CDW order is suppressed via hole substitution therefore stands to provide important insights into underlying or competing electronic instabilities and their roles in the unconventional coupling between CDW order and superconductivity reported in CsV_3Sb_5 .

Here we track the evolution of charge correlations in $\text{CsV}_3\text{Sb}_{5-x}\text{Sn}_x$ as holes are introduced via Sn-substitution and the parent $2 \times 2 \times 4$ CDW state is suppressed. X-ray diffraction data resolve that very light Sn-substitution ($x = 0.025$) suppresses interlayer correlations, and the CDW immediately becomes $2 \times 2 \times 2$ with short-range correlations along the c -axis. Increased hole-doping reveals the continued shortening of interlayer correlations and the eventual suppression of in-plane 2×2 CDW order; however, at concentrations where the parent CDW state is suppressed ($x = 0.15$), incommensurate quasi-1D charge correlations appear. Parallel STM measurements at this same composition also observe the persistence of low-temperature quasi-1D charge stripes in the absence of rotational symmetry breaking 2×2 CDW order [28]. Our data demonstrate an underlying electronic rotational symmetry breaking distinct from the broken rotational symmetry arising from the commensurate $2 \times 2 \times 4$ CDW state in the parent material, directly unveiling a complex landscape of charge correlations whose competition is reflected in the superconduct-

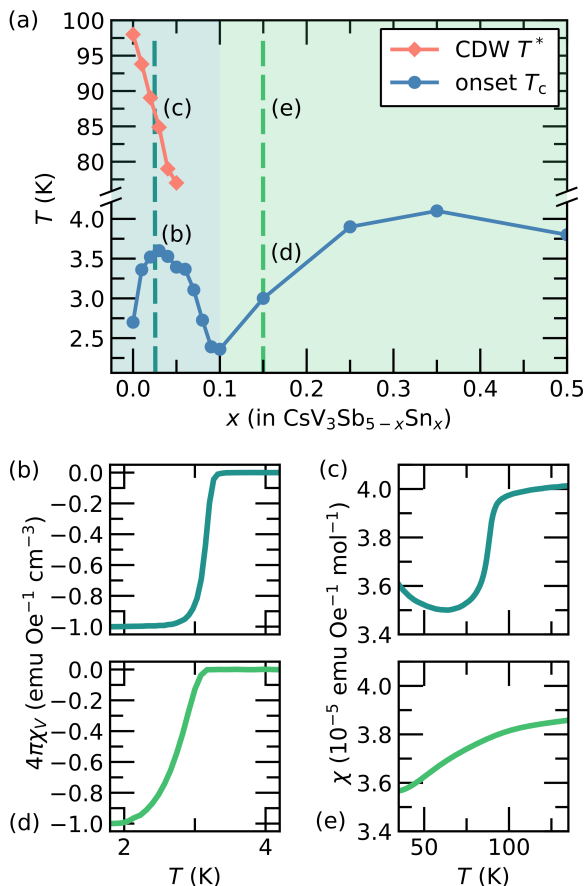


FIG. 1. (a) Electronic phase diagram of Sn-doped CsV_3Sb_5 showing the evolution of both CDW and SC order with hole-doping. Data are reproduced from Ref. [27]. Panels (b) and (c) show susceptibility data characterizing the superconducting and CDW states of the $x = 0.025$ composition in the first SC “dome” and panels (d) and (e) show susceptibility data characterizing the superconducting and CDW states of the $x = 0.15$ composition in the second SC “dome”.

ing transition temperature.

$\text{CsV}_3\text{Sb}_{5-x}\text{Sn}_x$ crystals with $x = 0.025$ and $x = 0.15$ were made with a flux of $\text{Cs}_{20}\text{V}_{15}\text{Sb}_{90}\text{Sn}_{30}$ and $\text{Cs}_{20}\text{V}_{15}\text{Sb}_{106}\text{Sn}_{34}$ respectively. Fluxes were ball-milled for 60 mins and then packed into alumina crucibles, and sealed under inert atmosphere within stainless steel tubes. Tubes were heated to 1000 °C and kept at 1000 °C for 12 hours and then cooled quickly to 900 °C, and then slowly cooled (2 °C / hour) to 500 °C. Temperature-dependent synchrotron x-ray diffraction were collected at the ID4B (QM2) beamline, CHESS. In ID4B measurements, temperature was controlled by a stream of cold helium gas flowing across the single-crystal sample. An incident x-ray of energy 26 keV ($\lambda = 0.6749$ Å) was selected using a double-bounce diamond monochromator. Bragg reflections were collected in transmission mode, and the sample was rotated with full 360° patterns, sliced into 0.1° frames. STM data were acquired using a

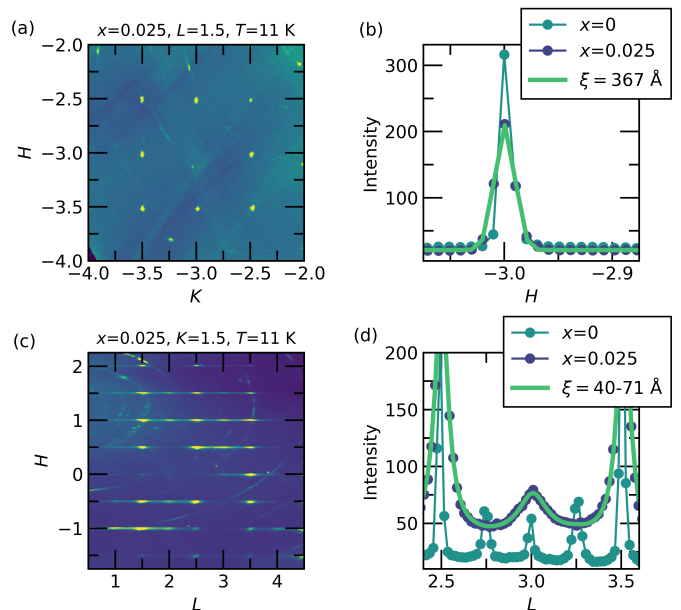


FIG. 2. (a) Map of x-ray scattering intensities in the $(H, K, 1.5)$ -plane for the $x = 0.025$ sample at $T = 11$ K. (b) One dimensional H -cuts through the $(-3, -2.5, 1.5)$ position for both $x = 0$ and $x = 0.025$. Solid lines are Gaussian fits to the data. (c) Map of x-ray scattering intensities in the $(H, 1.5, L)$ plane for the $x = 0.025$ sample. (d) One-dimensional L -cuts along $H=1$ for both the $x = 0$ and $x = 0.025$ samples. Solid lines are pseudo-Voigt fits for the $x = 0.025$ sample with the Gaussian component fixed to the instrument’s resolution.

Unisoku USM1300 STM at approximately 4.5 K. Spectroscopic measurements were made using a standard lock-in technique with 915 Hz frequency and bias excitation. STM tips were custom-made chemically-etched tungsten tips, annealed in UHV to bright orange color prior to the measurements.

To understand the evolution of charge correlations across the electronic phase diagram of $\text{CsV}_3\text{Sb}_{5-x}\text{Sn}_x$, two Sn concentrations were chosen as shown in Fig. 1 (a). The first $x = 0.025$ concentration possesses both a superconducting state with an enhanced T_c and a clearly observable CDW transition as shown in Figs. 1 (b) and (c). The second $x = 0.15$ concentration retains a SC phase transition but the thermodynamic signature of 2×2 CDW order in magnetization data has vanished as shown in Figs. 1 (d) and (e).

Looking first at the $x = 0.025$ crystal, maps of x-ray diffraction data were collected with representative data plotted in Figs. 2 (a) and (b). Fig. 2 (a) plots scattering within the $(H, K, 1.5)$ -plane. Reflections centered at $(H, K) = (0.5, 0.5)$ -type positions indicate that the 2×2 in-plane CDW order present in the undoped CsV_3Sb_5 remains in the $x = 0.025$ compound. Interlayer correlations are, however, altered. Fig. 2 (c) plots scattering within the $(H, 1.5, L)$ -plane, showing that c -axis corre-

lations shift to substantially shorter-range and center at the $L = 0.5$ position. This marks a switch into a quasi-2D $2 \times 2 \times 2$ CDW state from the long-range $2 \times 2 \times 4$ order of the undoped material and a transition into a CDW state whose \mathbf{q} vectors match those of undoped $(\text{K,Rb})\text{V}_3\text{Sb}_5$ [11].

The in-plane correlation lengths associated with CDW peaks in the $x = 0.025$ sample are slightly reduced, shortening from resolution-limited in the undoped material to $\xi_H = 367 \pm 6$ Å. Interplane correlation lengths shorten dramatically, moving from resolution-limited again in the undoped material to $\xi_L = 70 \pm 2$ Å. Weak reflections also persist at $L = \text{integer}$ positions with shorter correlation lengths $\xi_L = 40 \pm 2$ Å. The presence of these integer L reflections likely reflects that interlayer correlations continue to be heavily impacted by the nearly degenerate array of states along the U -line of the Brillouin zone [23, 29, 30], and the difference in correlation lengths between $L = 0.5$ and $L = 0$ type positions reflects two distinct patterns of order in the doped sample forming as it transitions to being truly quasi-2D.

At these small doping levels, while still in the CDW state, the immediate disappearance of $L=0.25$ type peaks upon small amounts of impurity/carrier substitution suggests a rapid crossover in the character of CDW order of CsV_3Sb_5 and a doping-induced switch from a state with modulating star-of-David and tri-Hexagonal order into one with phase shifted planes of a single distortion type, similar to $(\text{K,Rb})\text{V}_3\text{Sb}_5$ [20]. This crossover into another CDW phase at light doping may drive the formation of the first SC dome in the phase diagram of $\text{CsV}_3\text{Sb}_{5-x}\text{Sn}_x$; however a quantitative refinement of the intermediate $2 \times 2 \times 2$ CDW state will be required to further understand the mechanism.

Now examining charge correlations outside of the CDW phase boundary in the electronic phase diagram, x-ray scattering data for the $x = 0.15$ sample are plotted in Fig. 3. Panels (a) and (b) show a representative schematic of the scattering about the zone center and the corresponding data $(H, K, -0.5)$ -plane. Data collected at $\frac{1}{2}$ -integer L values indicate a superposition of three quasi-1D patterns of charge scattering, rotated 60° from one another in reciprocal space. This superposition of quasi-1D correlations can be understood in a model of charge correlations forming along one unique crystal axis (i.e. H or K), reducing the six-fold rotational symmetry of the lattice to two-fold, and forming three one-dimensional domains rotated by 120° in real space. This rotational symmetry breaking vanishes upon warming as shown in Fig. 3 (d), consistent with domain formation upon cooling.

Looking at scattering from a single quasi-1D domain, the charge correlations form an incommensurate state with $\mathbf{q}_{inc} = 0.37$ along a preferred in-plane axis. This is illustrated via a representative cut along H plotted in Fig. 3 (c). Within the (H, K) -plane, correlations along \mathbf{q}_{inc}

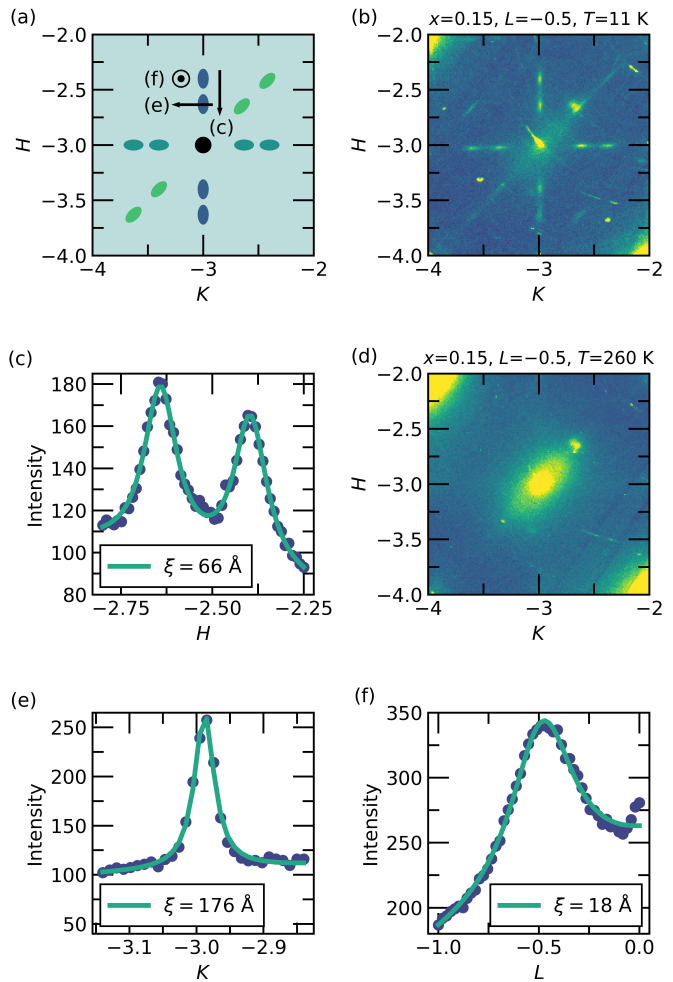


FIG. 3. (a) Schematic of x-ray scattering in the (H, K) -plane about a representative zone center for the $x = 0.15$ sample. Scattering from three domains is illustrated and cut directions for corresponding panels are labeled. (b) Map of x-ray scattering intensities for $x = 0.15$ at $T = 11$ K plotted about $(H, K, -0.5)$ (c) One dimensional cut along H as illustrated in panel (a), (d) Map of x-ray scattering intensities for $x = 0.15$ at $T = 300$ K (e-f) One dimensional cuts along K and L as illustrated in panel (a). Solid lines are the results of pseudoVoigt fits to the peak lineshapes with the Gaussian component constrained to the instrument's resolution.

are short-ranged with $\xi_H = 66 \pm 2$ Å and are substantially longer-ranged orthogonal to the direction of modulation with $\xi_K = 176 \pm 7$ Å (Fig. 2(e)). As shown in Fig. 3 (f), the peak of these quasi-1D correlations is centered at the $L = -0.5$ position with a short-correlation length of $\xi_L = 18 \pm 1$ Å, reflecting an anti-phase modulation between neighboring kagome layers correlated only between neighboring V-planes.

The appearance of incommensurate quasi-1D charge correlations following the collapse of 3D CDW order is suggestive of an underlying incommensurate and unidi-

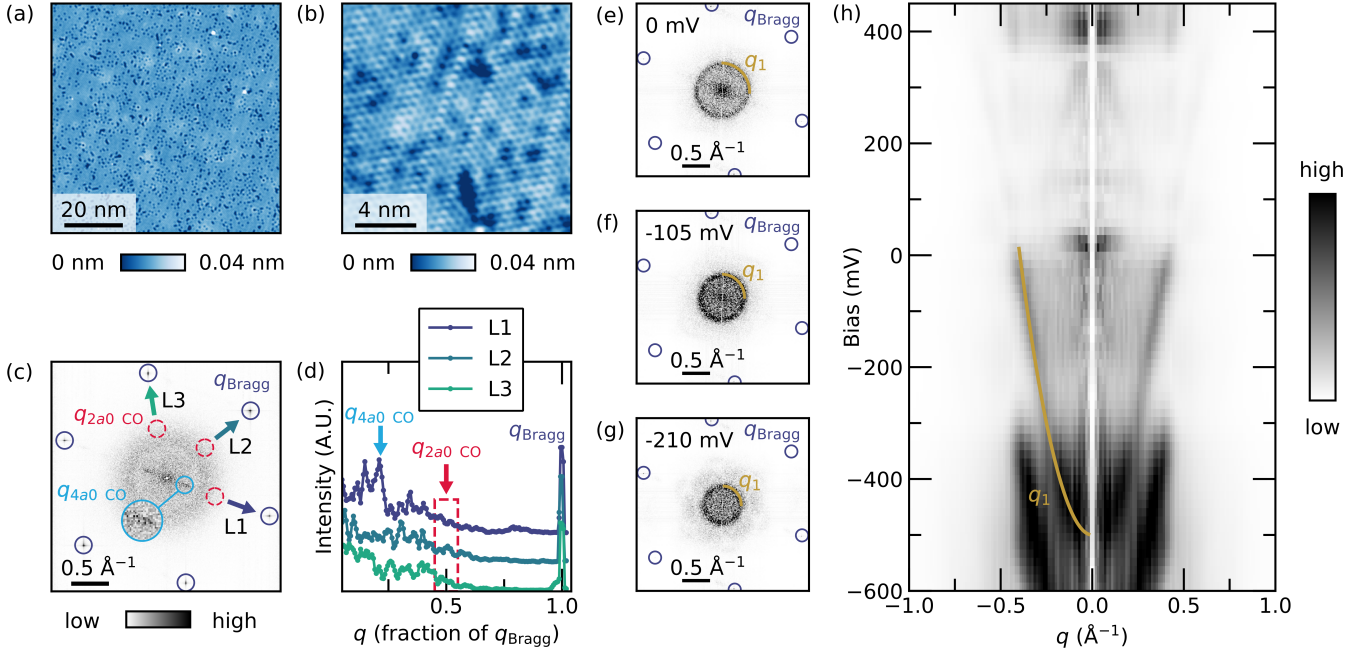


FIG. 4. (a) and (b) show STM topography images of CsV₃Sb₅, (c) Fourier transform of the STM topography showing the presence of $4a_0$ order and the absence of $2a_0$ correlations, (d) One dimensional line cuts through the Fourier map in panel (c), (e-g) Quasiparticle interference spectra collected at 0 mV, -105 mV, and -210 mV biases respectively. The circular scattering from q_1 due to the Sb p_z states is marked. (h) The dispersion of the QPI pattern showing the bottom of the Sb p_z band has risen to ≈ -500 meV.

rectional instability whose correlations compete with the parent 2×2 in-plane CDW order. Quasi-1D fluctuations were previously observed in STM measurements to onset well below T_{CDW} in undoped CsV₃Sb₅ [12], consistent with this notion of a nearby quasi-1D state. These fluctuations in the $x = 0$ system are locally pinned at the surface into a nearly commensurate surface phase and coherent, quasi-1D band features appear in the differential conductance dI/dV maps [31], reflective of a strong coupling between these fluctuations and the electronic structure.

To further investigate the local evolution of charge correlations, we perform STM measurements on the $x = 0.15$ sample at 4.5 K. Figs. 4 (a) and (b) show STM topographs of the Sb surface over different fields of view where dark hexagonal defects correspond to individual Sn dopants. Counting these defects is consistent with the expected Sn concentration of 0.15 Sn atoms per formula unit. One-dimensional, stripe-like features are apparent in the STM topograph (Figs. 4 (a) and (b)), which can be more easily quantified via the Fourier transform plotted in Fig. 4 (c). In this Fourier map, quasi-1D correlations are observed along one of the atomic Bragg peak directions, similarly to the previously identified $4a_0$ charge stripes in the $x = 0$ sample [12]. The superlattice peaks at the 2×2 (or $2a_0$) CDW positions are notably absent. This is further demonstrated via the line cuts through the

Fourier map along the three lattice directions, where no scattering peaks can be observed at $0.5Q_{Bragg}$ reciprocal space positions (Fig. 4 (d)).

To gain insight into the electronic band structure of the system, QPI imaging is plotted in Fig. 4. Fourier transforms of STM dI/dV maps in Figs. 4 (e)-(g) show the electron scattering and interference pattern as a function of increasing STM bias (binding energy). The dominant dispersive scattering wave vector is the nearly isotropic central circle (labeled q_1), which arises from scattering within the Sb p_z band that crosses through E_f . Hole-doping is predicted to be orbitally-selective and should preferentially dope this band [27, 32], pushing the bottom of the band closer to E_f . Figure 4 (h) shows the resulting dispersion of q_1 , where it can be seen that the bottom of the Sb p_z band has been pushed up from below -600 meV in the $x = 0$ parent system [12] to ≈ -500 meV in the $x = 0.15$ sample. This is consistent with DFT expectations of hole-doping achieved via the replacement of in-plane Sb atoms with Sn.

The persistence of quasi-1D charge correlations on the surface of the $x = 0.15$ sample in the absence of the 2×2 CDW state suggests that the fluctuations driving this surface order are robust to hole-doping and are likely linked to the incommensurate quasi-1D correlations that stabilize in x-ray scattering measurements once long-range CDW order is suppressed. The trade-off between the

two types of charge correlations in bulk x-ray measurements suggests that an underlying nematicity is operative across the electronic phase diagram of CsV_3Sb_5 (i.e. beyond where long-range CDW order vanishes). Our experiments establish AV_3Sb_5 as a promising platform for the studies of charge-stripe physics by scattering experiments and draw comparisons with the extensively studied $4a_0$ charge ordering in cuprates [33]. For example, the sizable doping dependence of charge ordering in Bi-based cuprates [34] appears qualitatively similar to what we have observed here in CsV_3Sb_5 with Sn doping. Given the suppression of charge ordering in cuprates in the overdoped regime, it will be of interest to explore the fate of 1D charge correlations in CsV_3Sb_5 at an even higher doping levels, as samples with higher Sn composition are developed in the future.

In summary, our results demonstrate a complex landscape of charge correlations in the hole-doped kagome superconductor $\text{CsV}_3\text{Sb}_{5-x}\text{Sn}_x$. Light hole-doping drives a transition into a neighboring CDW state with a $2 \times 2 \times 2$ supercell and short-range interlayer correlations. Doping further holes results in the suppression of the $3\mathbf{q}$ CDW state and the striking stabilization of quasi-1D, incommensurate charge correlations. These emergent quasi-1D correlations demonstrate an underlying electronic rotational symmetry breaking present across the phase diagram of this system and are suggestive of a $2k_f$ instability at the Fermi surface. Our results provide important experimental insights into neighboring/hidden charge correlations in the new class of AV_3Sb_5 superconductors and provide crucial input for modeling the unconventional interplay between charge density wave order and the low-temperature superconducting ground state.

ACKNOWLEDGMENTS

This work was supported by the National Science Foundation (NSF) through Enabling Quantum Leap: Convergent Accelerated Discovery Foundries for Quantum Materials Science, Engineering and Information (Q-AMASE-i): Quantum Foundry at UC Santa Barbara (DMR-1906325). I.Z. gratefully acknowledges the support from the National Science Foundation grant NSF-DMR-1654041. Z.W. is supported by U.S. Department of Energy, Basic Energy Sciences Grant No. DE-FG02-99ER45747 and the Cottrell SEED Award No. 27856 from Research Corporation for Science Advancement. The research reported here made use of shared facilities of the NSF Materials Research Science and Engineering Center at UC Santa Barbara DMR-1720256, a member of the Materials Research Facilities Network (www.mrfn.org). This work is based upon research conducted at the Center for High Energy X-ray Sciences (CHEXS) which is supported by the National Science Foundation under award DMR-1829070. Any opinions,

findings, and conclusions or recommendations expressed in this material are those of the authors and do not necessarily reflect the views of the National Science Foundation.

REFERENCES

-
- [1] B. R. Ortiz, L. C. Gomes, J. R. Morey, M. Winiarski, M. Bordelon, J. S. Mangum, I. W. Oswald, J. A. Rodriguez-Rivera, J. R. Neilson, S. D. Wilson, *et al.*, New kagome prototype materials: discovery of kv3sb5 , rbv3sb5 , and csv3sb5 , *Physical Review Materials* **3**, 094407 (2019).
 - [2] B. R. Ortiz, S. M. Teicher, Y. Hu, J. L. Zuo, P. M. Sarte, E. C. Schueller, A. M. Abeykoon, M. J. Krogstad, S. Rosenkranz, R. Osborn, *et al.*, Csv3sb5 : A z_2 topological kagome metal with a superconducting ground state, *Physical Review Letters* **125**, 247002 (2020).
 - [3] B. R. Ortiz, P. M. Sarte, E. M. Kenney, M. J. Graf, S. M. Teicher, R. Seshadri, and S. D. Wilson, Superconductivity in the z_2 kagome metal kv3sb5 , *Physical Review Materials* **5**, 034801 (2021).
 - [4] Q. Yin, Z. Tu, C. Gong, Y. Fu, S. Yan, and H. Lei, Superconductivity and normal-state properties of kagome metal rbv3sb5 single crystals, *Chinese Physics Letters* **38**, 037403 (2021).
 - [5] H. Chen, H. Yang, B. Hu, Z. Zhao, J. Yuan, Y. Xing, G. Qian, Z. Huang, G. Li, Y. Ye, *et al.*, Roton pair density wave in a strong-coupling kagome superconductor, *Nature* **599**, 222 (2021).
 - [6] J. Ge, P. Wang, Y. Xing, Q. Yin, H. Lei, Z. Wang, and J. Wang, Discovery of charge-4e and charge-6e superconductivity in kagome superconductor csv3sb5 , arXiv preprint arXiv:2201.10352 (2022).
 - [7] Y. Xu, Z. Ni, Y. Liu, B. R. Ortiz, S. D. Wilson, B. Yan, L. Balents, and L. Wu, Universal three-state nematicity and magneto-optical kerr effect in the charge density waves in av3sb5 ($a = \text{cs, rb, k}$), arXiv preprint arXiv:2204.10116 (2022).
 - [8] C. Mielke, D. Das, J.-X. Yin, H. Liu, R. Gupta, Y.-X. Jiang, M. Medarde, X. Wu, H. Lei, J. Chang, *et al.*, Time-reversal symmetry-breaking charge order in a kagome superconductor, *Nature* **602**, 245 (2022).
 - [9] L. Yu, C. Wang, Y. Zhang, M. Sander, S. Ni, Z. Lu, S. Ma, Z. Wang, Z. Zhao, H. Chen, *et al.*, Evidence of a hidden flux phase in the topological kagome metal csv3sb5 , arXiv preprint arXiv:2107.10714 (2021).
 - [10] C. Guo, C. Putzke, S. Konyzheva, X. Huang, M. Gutierrez-Amigo, I. Errea, D. Chen, M. G. Vergniory, C. Felser, M. H. Fischer, *et al.*, Field-tuned chiral transport in charge-ordered csv3sb5 , arXiv preprint arXiv:2203.09593 (2022).
 - [11] Y.-X. Jiang, J.-X. Yin, M. M. Denner, N. Shumiya, B. R. Ortiz, G. Xu, Z. Guguchia, J. He, M. S. Hossain, X. Liu, *et al.*, Unconventional chiral charge order in kagome superconductor kv3sb5 , *Nature Materials* **20**, 1353 (2021).
 - [12] H. Zhao, H. Li, B. R. Ortiz, S. M. Teicher, T. Park, M. Ye, Z. Wang, L. Balents, S. D. Wilson, and I. Zeljkovic, Cas-

- cade of correlated electron states in the kagome superconductor csv3sb5 , *Nature* **599**, 216 (2021).
- [13] N. Shumiya, M. S. Hossain, J.-X. Yin, Y.-X. Jiang, B. R. Ortiz, H. Liu, Y. Shi, Q. Yin, H. Lei, S. S. Zhang, *et al.*, Intrinsic nature of chiral charge order in the kagome superconductor rbv3sb5 , *Physical Review B* **104**, 035131 (2021).
- [14] T. Park, M. Ye, and L. Balents, Electronic instabilities of kagome metals: saddle points and landau theory, *Physical Review B* **104**, 035142 (2021).
- [15] H. Tan, Y. Liu, Z. Wang, and B. Yan, Charge density waves and electronic properties of superconducting kagome metals, *Physical review letters* **127**, 046401 (2021).
- [16] Z. Liang, X. Hou, F. Zhang, W. Ma, P. Wu, Z. Zhang, F. Yu, J.-J. Ying, K. Jiang, L. Shan, *et al.*, Three-dimensional charge density wave and surface-dependent vortex-core states in a kagome superconductor csv3sb5 , *Physical Review X* **11**, 031026 (2021).
- [17] B. R. Ortiz, S. M. Teicher, L. Kautzsch, P. M. Sarte, N. Ratcliff, J. Harter, J. P. Ruff, R. Seshadri, and S. D. Wilson, Fermi surface mapping and the nature of charge-density-wave order in the kagome superconductor csv3sb5 , *Physical Review X* **11**, 041030 (2021).
- [18] H. Li, T. Zhang, T. Yilmaz, Y. Pai, C. Marvinney, A. Said, Q. Yin, C. Gong, Z. Tu, E. Vescovo, *et al.*, Observation of unconventional charge density wave without acoustic phonon anomaly in kagome superconductors av3sb5 ($a = \text{rb, cs}$), *Physical Review X* **11**, 031050 (2021).
- [19] M. H. Christensen, T. Birol, B. M. Andersen, and R. M. Fernandes, Theory of the charge density wave in av3sb5 kagome metals, *Physical Review B* **104**, 214513 (2021).
- [20] M. Kang, S. Fang, J. Yoo, B. R. Ortiz, Y. Oey, S. H. Ryu, J. Kim, C. Jozwiak, A. Bostwick, E. Rotenberg, *et al.*, Microscopic structure of three-dimensional charge order in kagome superconductor av3sb5 and its tunability, *arXiv preprint arXiv:2202.01902* (2022).
- [21] Y. Hu, X. Wu, B. R. Ortiz, X. Han, N. C. Plumb, S. D. Wilson, A. P. Schnyder, and M. Shi, Coexistence of trihexagonal and star-of-david pattern in the charge density wave of the kagome superconductor av3sb5 , *arXiv preprint arXiv:2201.06477* (2022).
- [22] N. Ratcliff, L. Hallett, B. R. Ortiz, S. D. Wilson, and J. W. Harter, Coherent phonon spectroscopy and interlayer modulation of charge density wave order in the kagome metal csv3sb5 , *Physical Review Materials* **5**, L111801 (2021).
- [23] S. Wu, B. R. Ortiz, H. Tan, S. D. Wilson, B. Yan, T. Birol, and G. Blumberg, Charge density wave order in the kagome metal av3sb5 ($a = \text{cs, rb, k}$), *Physical Review B* **105**, 155106 (2022).
- [24] J. Luo, Z. Zhao, Y. Zhou, J. Yang, A. Fang, H. Yang, H. Gao, R. Zhou, and G.-q. Zheng, Possible star-of-david pattern charge density wave with additional modulation in the kagome superconductor csv3sb5 , *npj Quantum Materials* **7**, 1 (2022).
- [25] K. Chen, N. Wang, Q. Yin, Y. Gu, K. Jiang, Z. Tu, C. Gong, Y. Uwatoko, J. Sun, H. Lei, *et al.*, Double superconducting dome and triple enhancement of t_c in the kagome superconductor csv3sb5 under high pressure, *Physical Review Letters* **126**, 247001 (2021).
- [26] F. Yu, D. Ma, W. Zhuo, S. Liu, X. Wen, B. Lei, J. Ying, and X. Chen, Unusual competition of superconductivity and charge-density-wave state in a compressed topological kagome metal, *Nature communications* **12**, 1 (2021).
- [27] Y. M. Oey, B. R. Ortiz, F. Kaboudvand, J. Frassinetti, E. Garcia, R. Cong, S. Sanna, V. F. Mitrović, R. Seshadri, and S. D. Wilson, Fermi level tuning and double-dome superconductivity in the kagome metal csv3sb5-xsnx , *Physical Review Materials* **6**, L041801 (2022).
- [28] H. Li, H. Zhao, B. R. Ortiz, T. Park, M. Ye, L. Balents, Z. Wang, S. D. Wilson, and I. Zeljkovic, Rotation symmetry breaking in the normal state of a kagome superconductor kv3sb5 , *Nature Physics* **18**, 265 (2022).
- [29] Q. Xiao, Y. Lin, Q. Li, W. Xia, X. Zheng, S. Zhang, Y. Guo, J. Feng, and Y. Peng, Coexistence of multiple stacking charge density waves in kagome superconductor csv3sb5 , *arXiv preprint arXiv:2201.05211* (2022).
- [30] Q. Stahl, D. Chen, T. Ritschel, C. Shekhar, E. Sadrollahi, M. Rahn, O. Ivashko, M. v. Zimmermann, C. Felser, and J. Geck, Temperature-driven reorganization of electronic order in csv3sb5 , *Physical Review B* **105**, 195136 (2022).
- [31] H. Li, H. Zhao, B. Ortiz, Y. Oey, Z. Wang, S. D. Wilson, and I. Zeljkovic, Emergence of unidirectional coherent quasiparticles from high-temperature rotational symmetry broken phase of av3sb5 kagome superconductors, *arXiv preprint arXiv:2203.15057* (2022).
- [32] H. LaBollita and A. S. Botana, Tuning the van hove singularities in av3sb5 ($a = \text{k, rb, cs}$) via pressure and doping, *Physical Review B* **104**, 205129 (2021).
- [33] R. Comin and A. Damascelli, Resonant x-ray scattering studies of charge order in cuprates, *Annual Review of Condensed Matter Physics* **7**, 369 (2016), <https://doi.org/10.1146/annurev-conmatphys-031115-011401>.
- [34] E. H. da Silva Neto, P. Aynajian, A. Frano, R. Comin, E. Schierle, E. Weschke, A. Gyenis, J. Wen, J. Schneeloch, Z. Xu, *et al.*, Ubiquitous interplay between charge ordering and high-temperature superconductivity in cuprates, *Science* **343**, 393 (2014).